

Observation of fission residues in the $^{16}\text{O} + ^{181}\text{Ta}$ system at $E_{\text{lab}} \approx 6 \text{ MeV/A}$

Vijay R. Sharma^{1,a}, Abhishek Yadav¹, Pushpendra P. Singh², Devendra P. Singh¹, Manoj K. Sharma³, Unnati¹, R. Kumar⁴, B. P. Singh^{1,b}, R. Prasad¹, and A. K. Sinha⁵

¹Department of Physics, Aligarh Muslim University, Aligarh (U.P.)-202 002, India

²INFN-Laboratori Nazionali de Lagnaro, I-35020 Legnaro, Italy

³Physics Department, S. V. College, Aligarh (U.P.)-202 002, India

⁴NP- Group, Inter University Accelerator Centre (IUAC), New Delhi-110 067, India

⁵UGC-DAE-CSIR, Bidhan Nagar, Kolkata-700 098, India

Abstract. Present paper reports on the production cross-section of 24 fission like events ($30 \leq Z \leq 60$) formed via complete fusion-fission and/or incomplete fusion-fission processes in $^{16}\text{O}+^{181}\text{Ta}$ system at energies $\approx 6 \text{ MeV/A}$. Experiments have been performed using the recoil-catcher technique followed by off-line γ -spectroscopy. The measured cross-section of fission-like events is satisfactorily described by a statistical model code. Further, an attempt has been made to study the mass and isotopic yield distributions of fission fragments. The variance of the presently measured isotopic yield distributions has been found to be in agreement with the literature values for some other fissioning systems.

1 Introduction

Study of the interplay of fusion-fission processes in the heavy ion reactions has been an active area of investigation during the last decade. However, recent experimental data indicates the presence of nuclear fission even at low energies where the fusion is expected to be dominant [1-2]. On the basis of driving input angular momenta imparted into the system, the reactions may be categorized broadly into complete fusion (CF) and incomplete fusion (ICF) processes. Details of CF and/or ICF processes are given elsewhere [3]. Depending upon the beam energy and entrance channel mass asymmetry the compound nucleus formed as a result of CF and/or ICF may produce fragments which are characteristics of fission process. This is generally, referred to as complete fusion-fission (CFF) and/or incomplete fusion-fission (IFF). Nishio [4] has also reported that fission of incompletely fused composite nucleus is one of the dominant processes other than the fission of the composite system formed at intermediate energies. It has relevance in view of the fact that one of the most important observations in earlier studies was the discovery of asymmetric mass distribution in low energy fission of the majority of the actinides [5]. The asymmetric mass distribution may be explained on the basis of nuclear shell effects. Asymmetry in mass distribution decreases with the increase in excitation energy. In view of the above, the study of the dynamics of heavy ion (HI) collisions [6,7] and systematic studies

of the competition of various reaction processes which contribute to the total cross sections are of considerable importance.

In order to study the dynamics of the processes in the $^{16}\text{O} + ^{181}\text{Ta}$ system, a programme has been undertaken by our group. In the first part of the experiment, excitation functions for a large number of reactions in this system were analysed to study the CF and ICF processes in the energy range $\approx 76\text{-}100 \text{ MeV}$ [8]. Further, experimental study for the same system has been done to interpret the competition between CF and/or ICF through recoil range distribution (RRD) measurements [8]. A part of the data analysis involving observation of fission events is reported in this paper. To the best of our knowledge these measurements in the $^{16}\text{O}+^{181}\text{Ta}$ system have been done for the first time.

2 Experimental Details

Experiment has been performed using $^{16}\text{O}^{7+}$ beam from 15UD pelletron accelerator at the Inter-University Accelerator Centre (IUAC), New Delhi, India. The thin target foils of isotopically pure (99.9%) Tantalum and Al-catchers were prepared using rolling technique. The thickness of each target and catcher foil was determined by α -transmission method. The thicknesses of the samples were determined from the observed change in the energy of the α -particles by using standard stopping power values [9] and were found to be $\approx 1.5 \text{ mg/cm}^2$ for Ta-targets and $\approx 2.0 \text{ mg/cm}^2$ for Al-catchers. The

^aphy.vijayraj@gmail.com, ^bbpsinghamu@gmail.com

thickness of the Al-catchers was chosen keeping in view the fact that even the most energetic residues produced due to the complete momentum transfer (CMT) may be trapped in the catcher thickness. It may be pointed out that recoil energy of the composite system (^{197}Tl) formed as a result of CMT in $100\text{ MeV } ^{16}\text{O}+^{181}\text{Ta}$ is $\approx 8\text{ MeV}$. The range of these $\approx 8\text{ MeV}$ heavy residues in Al is $\approx 0.408\text{ mg/cm}^2$. As such, they are completely stopped in the catcher thickness used in the present work. The ^{181}Ta -foil samples and Al-catchers were cut into $1.2 \times 1.2\text{ cm}^2$ size and pasted on Al-holders having concentric holes of 1.0 cm diameter. Each target was followed by Al-catcher. The Al-holders were used for the rapid dissipation of heat produced during the irradiation. The irradiation has been carried out in the General Purpose Scattering Chamber, of 1.5 m diameter having in-vacuum transfer facility, with a beam current $\approx 10\text{ pA}$. A sketch of typical experimental set up is shown in Fig 1. The beam energy incident on the first target was 100 MeV . After an energy loss of $\approx 3\text{ MeV}$, while passing through first target-catcher assembly the beam energy incident on second ^{181}Ta target was $\approx 97\text{ MeV}$. Thus, in a single bombardment, two samples are irradiated. Keeping in view the half-lives of interest, irradiations have been carried out for $\approx 8\text{ hours}$. The beam flux was monitored using an ORTEC current integrator by taking into account the charge collected in the Faraday cup, placed behind the stack of target-catcher assembly. The activities

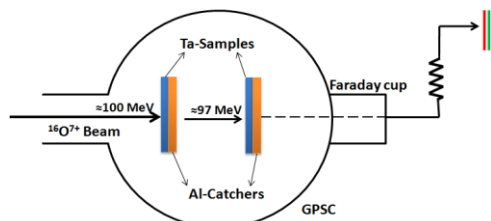


Fig.1. Sketch of a typical experimental set-up used for the irradiation.

produced in the samples were recorded off-line by HPGe detector of 100 c.c. active volume coupled to a CAMAC based software FREEDOM [10]. The detector used in this experiment was pre-calibrated for energy and efficiency using various standard γ -sources viz., ^{60}Co , ^{133}Ba and ^{152}Eu at different source-detector separations. The target-detector separation was suitably adjusted so as to keep the dead time $< 10\%$. In order to detect and follow the residues of longer half-lives, the counting of irradiated samples has been done for a week or so. Further experimental details along with the factors that may introduce uncertainties in the measured cross-sections are given elsewhere [11]. However, the overall errors in the measured cross-section are estimated to have uncertainties $< 15\%$.

3 Measurements and Analysis

Our earlier studies [8] have indicated that the dominant CF and/or ICF residues produced in the interaction of $^{16}\text{O}+^{181}\text{Ta}$ system are $^{194g,194m,193g,193m,192g,192m}\text{Tl}$, $^{193g,193m,192,191g,191m}\text{Hg}$ and $^{192g,191g,190g}\text{Au}$. Analysis of the experimental data done in the present work on $^{16}\text{O} + ^{181}\text{Ta}$

system revealed the presence of several residues which are not expected to be populated either by CF and/or ICF processes. Moreover, these residues were found to have charge and atomic mass values around half of the values for the residues produced by composite systems formed as a result of fusion of projectile and the target nucleus, indicating the possibility of their production only through fission of composite systems. It may be pointed out that these residues were identified not only by their characteristic γ -rays but also from their measured half lives. As a typical example the decay curve for the

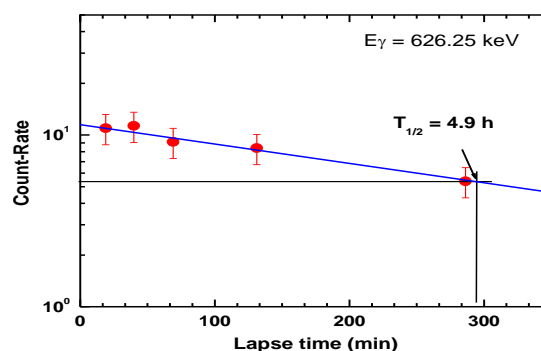


Fig. 2 A typical decay curve of Indium residue at $E_{\text{Lab}} \approx 100\text{ MeV}$

Indium (^{110}In) residue identified by $\approx 626\text{ keV}$ γ -ray and $\approx 4.9\text{ h}$ half-life ($T_{1/2}$) is shown in Fig 2. The measured half-lives of all the fission like residues were found to be in good agreement with their literature values [12]. A list of fission fragments identified in the present work, their γ -ray energies, abundances etc., are given elsewhere [11]. In the present work, 24 fission fragments formed as a result of fusion-fission processes have been identified. These residues may be formed (a) by the direct fission of the CF and/or ICF residues (first chance fission) and/or (b) by the fission of CF and/or ICF after emission of a few nucleons (second, third, etc. chance fission). The cross-sections for the population of these residues were determined from the intensities of the characteristic γ -lines of the fission residues using the standard formulation [2]. Measured cross-sections for the identified fission fragments both at 97 and 100 MeV beam energies are given in table 1. It may be pointed out that, the measured cross-sections data for a given fission fragment is the cumulative sum of its population from various decay chains that may lead to the same final product [11].

3.1 Isotopic Yield Distribution

In general, for heavy composite systems at moderate excitation energies nucleon emission competes directly with fission. The emission of higher charged particles is severely hindered because of the large Coulomb barrier. In such cases, nucleon emission from the fission fragments and/or the fission of successive elements of fission chains, may give rise to the isotopic and isobaric distributions of fission residues. However, as compared to proton emission, the emission of neutrons is more probable and therefore, in most of the cases only the

Table 1. Measured cross-section of the final fission residues via CFF and/or IFF at 97 and 100 MeV, respectively.

S. No.	Residues	σ (mb) ≈ 97 MeV	σ (mb) ≈ 100 MeV
1.	^{71}Zn	1.3 \pm 0.03	2.6 \pm 0.03
2.	^{75}Ge	25.4 \pm 0.90	23.6 \pm 0.65
3.	^{77}Kr	-	6.5 \pm 0.23
4.	$^{85\text{m}}\text{Y}$	26.2 \pm 2.45	27.4 \pm 0.55
5.	^{86}Y	60.6 \pm 8.56	86.1 \pm 12.38
6.	^{88}Kr	25.4 \pm 0.12	46.8 \pm 0.44
7.	$^{90\text{m}}\text{Y}$	1.5 \pm 0.42	2.3 \pm 0.65
8.	$^{91\text{m}}\text{Y}$	0.9 \pm 0.58	1.5 \pm 0.87
9.	^{93}Y	-	10.4 \pm 1.56
10.	^{105}Ru	21.5 \pm 0.06	46.9 \pm 0.35
11.	^{105}In	-	17.83 \pm 3.6
12.	^{110}In	57.5 \pm 0.61	56.2 \pm 6.52
13.	$^{110\text{m}}\text{In}$	1.0 \pm 0.03	1.3 \pm 0.25
14.	$^{111\text{m}}\text{In}$	-	3.5 \pm 0.6
15.	$^{113\text{m}}\text{In}$	-	1.22 \pm 0.64
16.	^{117}Cd	24.2 \pm 0.18	31.0 \pm 0.59
17.	^{117}Sb	10.9 \pm 0.01	19.6 \pm 1.21
18.	^{121}Xe	26.6 \pm 0.11	32.3 \pm 0.50
19.	^{129}Sb	4.8 \pm 0.03	5.3 \pm 0.12
20.	^{132}La	-	4.5 \pm 2.18
21.	^{132}Ce	16.5 \pm 0.40	39.8 \pm 1.11
22.	$^{132\text{m}}\text{I}$	-	1.6 \pm 0.38
23.	^{137}Nd	7.7 \pm 0.04	25.6 \pm 0.15
24.	^{141}Sm	3.0 \pm 0.15	5.7 \pm 0.37

isotopic yield distributions is experimentally observed. As a representative case experimentally determined isotopic yield distributions for Indium ($^{105,110,111\text{m},113\text{m}}\text{In}$) isotopes at 100 MeV are plotted in Fig 3. Since, only the metastable states of $^{111\text{m},113\text{m}}\text{In}$ for Indium isotopes have been measured, the total production cross-section for these isotopes will be higher than the values shown, which is indicated by upward arrows (see Fig 3). The isotopic yield distribution has been fitted to a Gaussian using the prescription given in ref. [11]. The value of chi square (χ^2) was minimized, keeping the width parameter σ_A and most probable mass A_P as free parameters in peak fitting software.

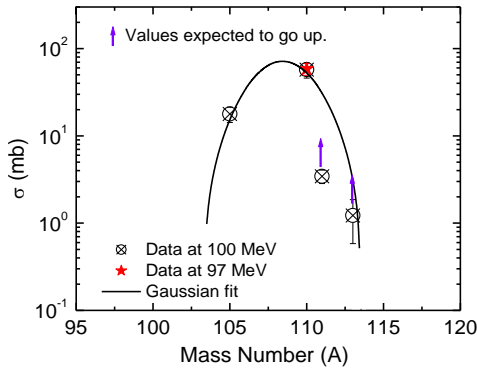


Fig.3. Isotopic Yield Distribution for ($^{105,110,111\text{m},113\text{m}}\text{In}$) Indium isotopes in $^{16}\text{O} + ^{181}\text{Ta}$ reaction at 100 MeV.

As a typical example for In isotopes the value of most probable mass $A_P \approx 108.42$ and of width parameter ($\sigma_A \approx 2.08$) obtained in the present work compares well with the corresponding values of 107.88 and 2.06 reported, for $^{16}\text{O} + ^{169}\text{Tm}$ system at $E/A \approx 5.9$ MeV, obtained by Singh

et al. [2]. Furthermore, the variance σ_A^2 reported in literature for a large number of other fissioning systems are shown in table 2, along with the value obtained for the present work. As can be seen from this table, the σ_A^2 values determined in the present work are close to the literature values for some other fissioning systems. It may be pointed out that the Gaussian distribution of isotopic mass distribution has been observed at the excitation energy ≈ 67 MeV corresponding to 100 MeV incident energy. However, at the lower incident energy (≈ 97 MeV) only few isotopes were identified and therefore, their distribution could not be studied.

Table 2. Comparison of the variance (σ_A^2) of the isotopic yield distribution for different fissioning systems.

System	Excitation energy E^* (MeV)	Element	σ_A^2
$^{16}\text{O} + ^{181}\text{Ta}$	67.041	Y	3.03
$^{16}\text{O} + ^{181}\text{Ta}$	67.041	In	4.32
$^{16}\text{O} + ^{169}\text{Tb}$ [2]	57.1	Sr	3.31
$^{16}\text{O} + ^{169}\text{Tb}$ [2]	57.1	Y	4.41
$^{16}\text{O} + ^{159}\text{Tm}$ [2]	61.06	In	4.24
$^{16}\text{O} + ^{159}\text{Tm}$ [2]	61.06	Tc	4.62
$^7\text{Li} + ^{232}\text{Th}$ [22]	41.7	Sb	4.08
$^7\text{Li} + ^{232}\text{Th}$ [22]	41.7	I	3.96
$^{11}\text{B} + ^{232}\text{Th}$ [23]	55.7	Sb	4.0
$^{11}\text{B} + ^{232}\text{Th}$ [23]	55.7	I	5.43
$^{11}\text{B} + ^{232}\text{Th}$ [23]	55.7	Cs	3.72
$^{11}\text{B} + ^{238}\text{U}$ [24]	67.4	Rb	3.84
$^{11}\text{B} + ^{238}\text{U}$ [24]	67.4	Cs	3.95

3.2 Mass Distribution

Mass distribution is one of the important observables directly related to the collective dynamics of fission process [13]. Cross-sections obtained from the activities measured in the target-catcher assembly were used for the mass distribution studies. The plots of experimentally determined production cross-sections (given in table 1) of various fission fragments at two different energies ($E_{\text{lab}} \approx 97$ MeV and 100 MeV) are shown in Fig.4 (a) and (b), respectively. The upward arrows indicate that only the metastable states have been measured and the total production cross-sections of these fission fragments are expected to increase. These distributions have been found to be symmetric, in general, as expected. Stability (stiffness) of the fissioning nucleus to mass-asymmetric deformation can be understood through observed mass distribution. In order to understand this aspect Itkis *et al.* [14] analysed a large collection of data over a wide range of fissility of compound nucleus at medium excitation energies. The variance of the mass distribution obtained in the present have been compared for the same projectile (^{16}O) and different targets as a function of mass asymmetry ($\mu = M_T/M_{T+P}$) of interacting systems, taken from literature [15-18] and are shown as a bar diagram in Fig. 5. It may be observed from Fig.5, that variance of mass distribution increases with the mass asymmetry of the interacting ions. Further, the total experimental fission cross section (σ_F^T) has been obtained by adding the measured cross-sections for individual fission

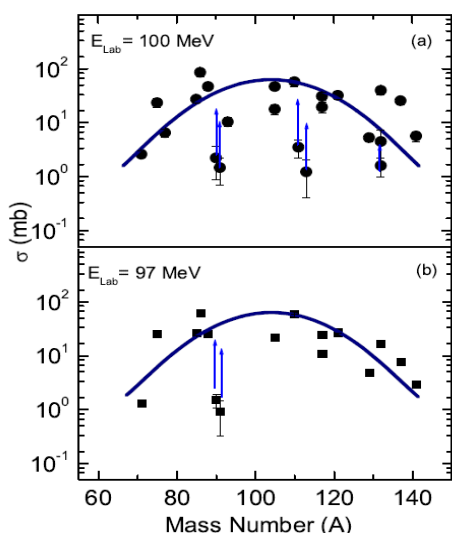


Fig.4. The plots of experimentally determined production cross-sections of various fission fragments at two different energies.

fragments. The value of σ_F^T at ≈ 97 and 100 MeV beam energies are found to be ≈ 315 mb and ≈ 500 mb. The total fission cross-section has also been theoretically estimated using statistical code ALICE [19], which employs a rotating liquid drop model [20]. The calculated σ_F^T values are found to be ≈ 500 mb and ≈ 680 mb at energies 97 MeV and 100 MeV, respectively which is in reasonable agreement with the experimentally measured fission cross-sections. Gilmore *et al.* [21] has also measured total fission cross-section for the same system employing emulsion technique. From the analysis of their data [21] they obtained the total fission cross-sections ≈ 300 mb and ≈ 430 mb at 97 MeV and 100 MeV, respectively which, in general, agree within experimental errors to the values obtained in the present work. However, it may be pointed out that the resolution and the detection efficiency of the present measurements are significantly better than that of earlier work [21].

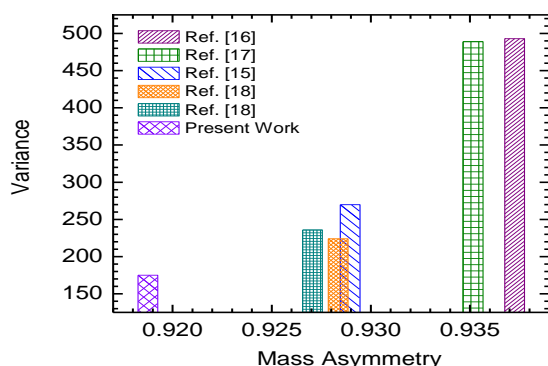


Fig.5. Bar diagram of mass asymmetry vs variances for same projectile and different target combination.

4 Summary and Conclusions

In the present work several fission fragments populated via CFF and/or IFF processes in $^{16}\text{O}+^{181}\text{Ta}$ system at 97 MeV and 100 MeV have been identified and their production cross-sections have been obtained. The data has been analyzed to deduce parameters of isotopic yield

distributions. Mass distribution of fission fragments has also been obtained. The isotopic yield distributions are satisfactorily reproduced by Gaussian distribution. The distribution parameters obtained from the present measurements agree reasonably well with the literature values. The total fission cross section obtained from the present measurements agrees with some earlier measurements as well as with those calculated using angular momentum dependent rotating liquid drop fission barrier. An online experiment employing the fission detectors, by measuring the neutron multiplicity using the neutron array setup is proposed to get a detailed insight of fission dynamics for the system.

5 Acknowledgements

The authors thank to the Chairman, Department of Physics, and the Director, IUAC, New Delhi, India for providing all the necessary facilities to carry out the experiment and analysis. BPS and RP thank the UGC/DST for support.

References

1. L. Corradi, Journal of Physics, Conference Series **282**, 012005 (2011)
2. Pushpendra P. Singh *et al.*, Int. J. M. Phys. E, Vol. 17, No. 3 549-566 (2008)
3. Pushpendra P. Singh *et al.*, Phys. Lett. B **671**, 20–24 (2009)
4. K. Nishio *et al.*, Phys. Rev. Lett. **93**, 162701 (2004)
5. R. Tripathi *et al.*, Euro. Phys. J. A **26**, 271 (2005)
6. R. L. Kozub *et al.*, Phys. Rev. C **11**, 1497 (1975)
7. J. B. Natowitz, E. T. Chulick, and M. N. Namboodiri, Phys. Rev. C **6**, 2133 (1972)
8. Devendra P. Singh *et al.*, Phys. Rev. C **80**, 014601 (2009), Phys. Rev. C **81**, 054607 (2010)
9. SRIM06; <http://www.srim.org/>
10. FREEDOM: Data Acquisition and Analysis System designed at the Inter University Accelerator Centre, New Delhi, India
11. Vijay R. Sharma, M. Phil. Dissertation (2011), A. M. U., Aligarh, INDIA, unpublished.
12. E. Brown and R. B. Firestone, Table of Isotopes, Wiley, New York, 1986.
13. A. C. Berriman, D. J. Hinde, M. Dasgupta and J. O. Newton, Nature (London) **413**, 144 (2001)
14. M. G. Itkis *et al.*, Phys. At. Nucl. **58**, 2026 (1995)
15. L. M. Pant *et al.*, Eur. Phys. J. A **11**, 47 (2001)
16. W. Q. Shen *et al.*, Phys. Rev. C **36**, 115 (1987)
17. A. Goswami *et al.*, Radiochem. Acta **62**, 173 (1993)
18. M. G. Itkis *et al.*, in European Physical Society XV Nucl. Phys. Divisional Conference on Low Energy Nuclear Dynamics, (World Scientific, Singapore, 1995), p. 177
19. F. Plasil and M. Blann, Phys. Rev. C **11**, 508 (1975)
20. S. Cohen *et al.*, Ann. Phys. (N.Y.) **82**, 557 (1974)
21. Gilmore *et al.*, Phys. Rev. **128**, N (1962)
22. R. Tripathi *et al.*, Radiochem. Acta **90** 185 (2002)
23. G. K. Gubbi *et al.*, Phys. Rev. C **59** 3224 (1999)
24. M. de *et al.*, Phys. Rev. C **14** 2185 (1976)